

# Latest BEM developments and The microwave and sub-millimetre database

December 2020

Antigoni Kleanthous, University College London, UK

Timo Betcke, University College London, UK

David Hewett, University College London, UK

Anthony Baran, The Met Office, UK & University of Hertfordshire, UK



# Part I: Accelerated Calderón preconditioning for Maxwell transmission problems

Antigoni Kleanthous, University College London, UK

Timo Betcke, University College London, UK

David Hewett, University College London, UK

Paul Escapil-Inchauspé, Universidad Adolfo Ibáñez, Santiago, Chile

Carlos Jerez-Hanckes, Pontificia Universidad Católica de Chile, Santiago, Chile

Anthony Baran, The Met Office, UK & University of Hertfordshire, UK

# The Boundary Element Method (BEM)

- Reformulate the problem into boundary integral equations on the boundary of the scatterer
- Discretise the boundary and transform the boundary integral equations into a matrix system
- Solve the discrete problem on the boundary using an iterative solver
- The solution on the boundary can be extended to the interior/exterior/far field area through representation formulae

# Why use BEM?

- Reduces the dimensionality of the problem from a 3D domain to a 2D manifold
  - Discretisation is easier/faster
  - The matrix system is smaller
- Radiation conditions at infinity automatically satisfied
- Can solve the full time-harmonic Maxwell problem without the need for any approximations
- Can handle complicated domains – ideal for complex shaped ice crystals

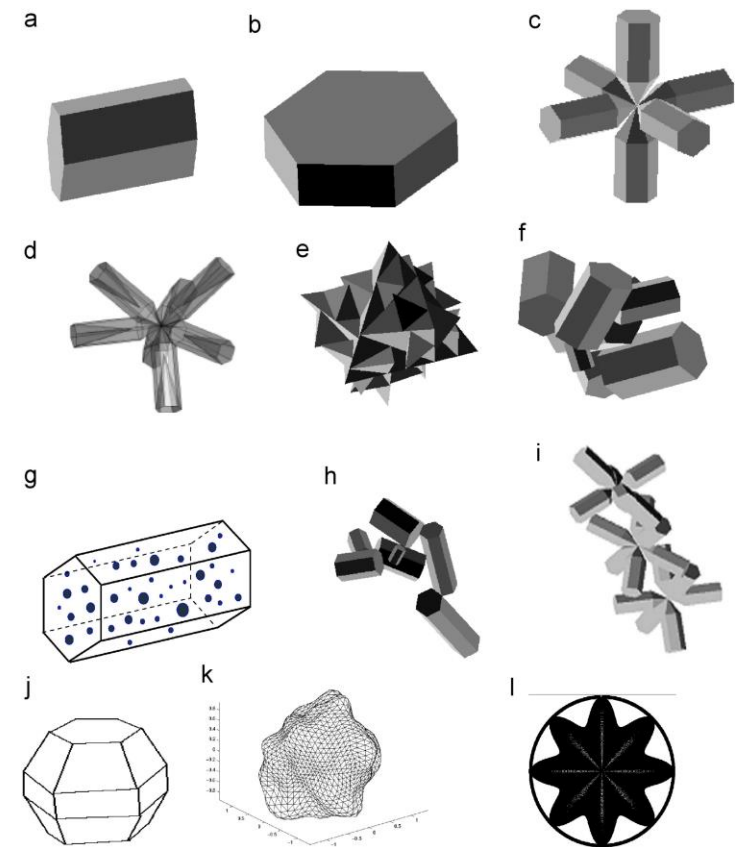


Image taken from: Baran, Anthony J. "A review of the light scattering properties of cirrus." Journal of Quantitative Spectroscopy and Radiative Transfer 110.14-16 (2009): 1239-1260.

# Bempp

Boundary element method Python package

**HOME**

**INSTALLATION**

**DOCUMENTATION**

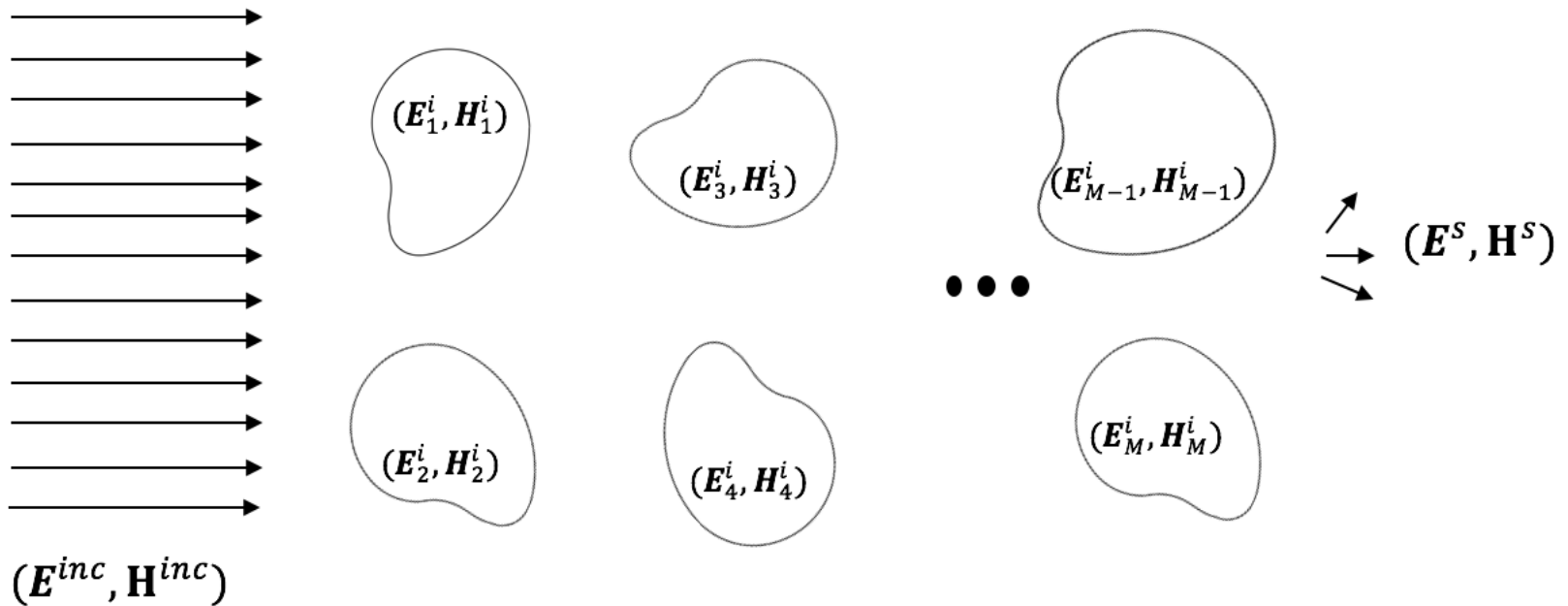
**PUBLICATIONS**

**SUPPORT**

Bempp is an open-source computational boundary element platform to solve electrostatic, acoustic and electromagnetic problems. Features include:

- Easy-to-use Python interface.
- Support for triangular surface meshes.
- Import and export in a number of formats, including Gmsh and VTK.
- Easy formulation of acoustic and electromagnetic transmission problems.
- CPU and GPU parallelisation.
- A comprehensive operator algebra that makes it easy to formulate complex product operator formulations such as operator preconditioning.
- Coupled FEM/BEM computations via interfaces to [FEniCS](#).

# The scattering problem



# The scattering problem

- $(\mathbf{E}_m^i, \mathbf{H}_m^i)$  and  $(\mathbf{E}^e, \mathbf{H}^e)$ : interior and exterior fields with

$$\mathbf{E}^e = \mathbf{E}^{inc} + \mathbf{E}^s, \quad \mathbf{H}^e = \mathbf{H}^{inc} + \mathbf{H}^s,$$

- Time-harmonic Maxwell equations

$$\begin{aligned}\nabla \times \mathbf{E}_m^i &= i\omega\mu_m \mathbf{H}_m^i, & \nabla \times \mathbf{H}_m^i &= -i\omega\epsilon_m \mathbf{E}_m^i, & \text{in } \Omega_m^i, \\ \nabla \times \mathbf{E}^e &= i\omega\mu_e \mathbf{H}^e, & \nabla \times \mathbf{H}^e &= -i\omega\epsilon_e \mathbf{E}^e & \text{in } \Omega^e,\end{aligned}$$

- Transmission boundary conditions

$$\mathbf{E}_m^i(\mathbf{x}) \times \mathbf{n} = \mathbf{E}^e(\mathbf{x}) \times \mathbf{n}, \quad \mathbf{H}_m^i(\mathbf{x}) \times \mathbf{n} = \mathbf{H}^e(\mathbf{x}) \times \mathbf{n}, \quad \mathbf{x} \in \Gamma_m.$$

# The scattering problem

- $(\mathbf{E}_m^i, \mathbf{H}_m^i)$  and  $(\mathbf{E}^e, \mathbf{H}^e)$ : interior and exterior fields with

$$\mathbf{E}^e = \mathbf{E}^{inc} + \mathbf{E}^s, \quad \mathbf{H}^e = \mathbf{H}^{inc} + \mathbf{H}^s,$$

- Time-harmonic Maxwell equations

$$\nabla \times (\nabla \times \mathbf{E}_m^i) - k_m^2 \mathbf{E}_m^i = 0, \quad \text{in } \Omega_m^i,$$

$$\nabla \times (\nabla \times \mathbf{E}^e) - k_e^2 \mathbf{E}^e = 0, \quad \text{in } \Omega^e,$$

- Transmission boundary conditions

$$\mathbf{E}_m^i(\mathbf{x}) \times \mathbf{n} = \mathbf{E}^e(\mathbf{x}) \times \mathbf{n}, \quad \mathbf{x} \in \Gamma_m.$$

# The PMCHWT formulation

$$\mathcal{A}\mathbf{u}^s = \left( \frac{1}{2}\mathcal{I} - \mathcal{A}^i \right) \mathbf{u}^{inc}$$

$$\mathcal{A} = \begin{bmatrix} \mathcal{A}_1^e + \mathcal{A}_1^i & \mathcal{A}_{12} & \cdots & & \mathcal{A}_{1M} \\ \vdots & \ddots & \ddots & & \vdots \\ \mathcal{A}_{21} & \ddots & \ddots & \ddots & \vdots \\ \vdots & \ddots & \ddots & \ddots & \vdots \\ & & & \ddots & \mathcal{A}_{(M-1)M} \\ \mathcal{A}_{M1} & \cdots & \mathcal{A}_{M(M-1)} & \mathcal{A}_M^e + \mathcal{A}_M^i & \end{bmatrix}, \quad \mathcal{A}^i = \begin{bmatrix} \mathcal{A}_1^i & 0 & \cdots & 0 \\ \vdots & \ddots & \ddots & \vdots \\ 0 & \ddots & \ddots & \vdots \\ \vdots & \ddots & \ddots & 0 \\ 0 & \cdots & 0 & \mathcal{A}_M^i \end{bmatrix},$$

$$\mathcal{I} = \begin{bmatrix} \mathcal{I}_1 & 0 & \cdots & 0 \\ \vdots & \ddots & \ddots & \vdots \\ 0 & \ddots & \ddots & 0 \\ \vdots & \ddots & \ddots & \vdots \\ 0 & \cdots & 0 & \mathcal{I}_M \end{bmatrix}, \quad \mathbf{u}^s = \begin{bmatrix} \mathbf{u}_1^s \\ \mathbf{u}_2^s \\ \vdots \\ \mathbf{u}_M^s \end{bmatrix}, \quad \mathbf{u}^{inc} = \begin{bmatrix} \mathbf{u}_1^{inc} \\ \mathbf{u}_2^{inc} \\ \vdots \\ \mathbf{u}_M^{inc} \end{bmatrix}.$$

# Calderón Preconditioning

$$\mathcal{A}^2 \mathbf{u}^s = \mathcal{A} \left( \frac{1}{2} \mathcal{I} - \mathcal{A}^i \right) \mathbf{u}^{inc}$$

Cools, Kristof, Francesco P. Andriulli, and Eric Michielssen. "A Calderón multiplicative preconditioner for the PMCHWT integral equation." *IEEE transactions on Antennas and Propagation* 59.12 (2011): 4579-4587.

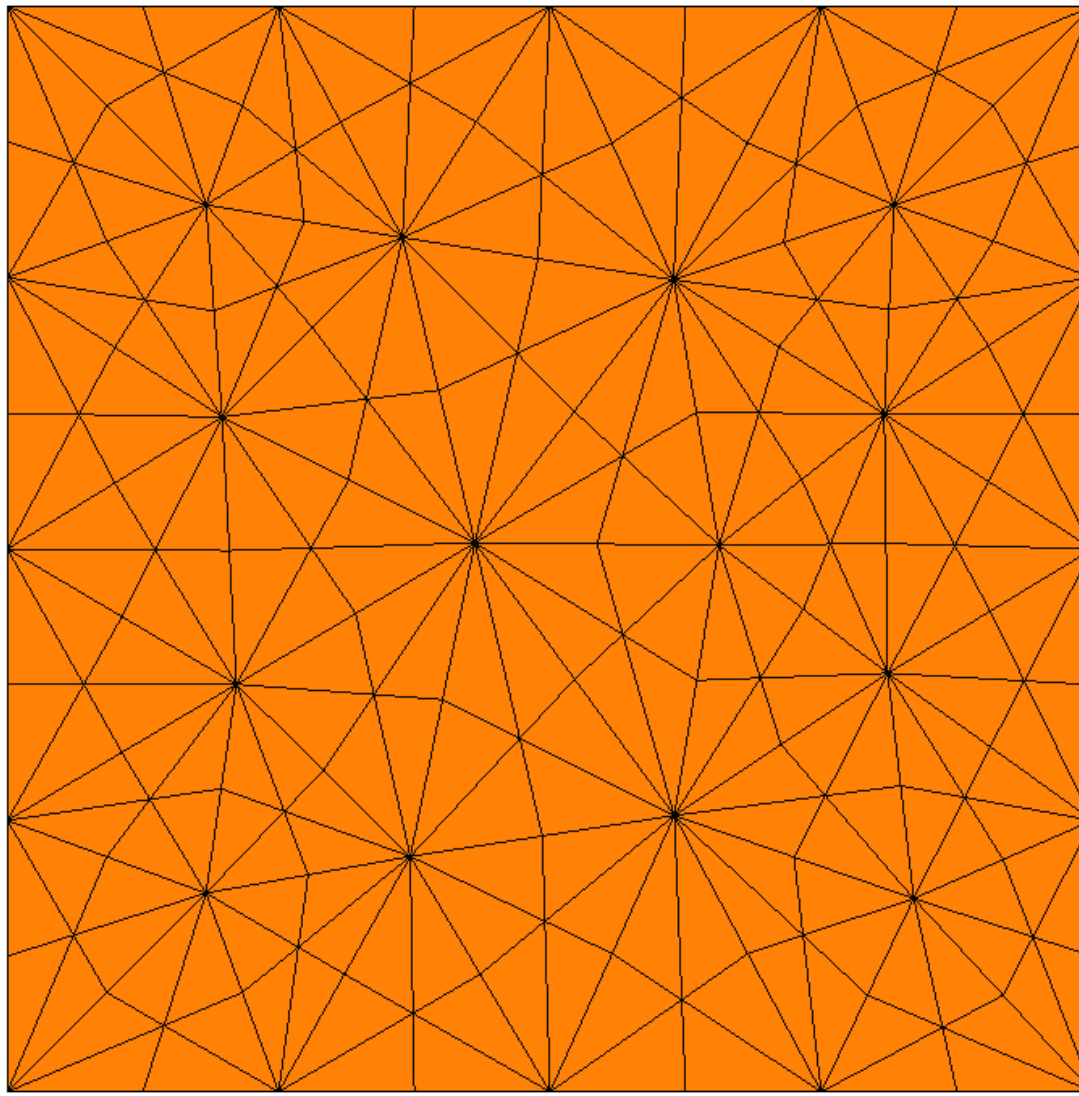
Kleanthous, Antigoni, et al. "Calderón preconditioning of PMCHWT boundary integral equations for scattering by multiple absorbing dielectric particles." *Journal of Quantitative Spectroscopy and Radiative Transfer* 224 (2019): 383-395.

# Accelerated Preconditioning

- To accurately capture the wave solution a mesh refinement of 10 elements per wavelength is usually used
- To stably discretise the operator product PA, the use of a dual mesh is required. The dual mesh is defined on the barycentrically refined original mesh leading to a 6-fold increase in the number of elements
- Applications have been limited to relatively small size parameters due to memory and time constraints.
- Accelerating techniques to reduce memory and assembly time

Kleanthous, Antigoni, et al. "Calderón preconditioning of PMCHWT boundary integral equations for scattering by multiple absorbing dielectric particles." Journal of Quantitative Spectroscopy and Radiative Transfer 224 (2019): 383-395.

Kleanthous, Antigoni, et al. "Accelerated Calderón preconditioning for Maxwell transmission problems." arXiv preprint arXiv:2008.04772 (2020).



Y  
Z X

# Accelerated Preconditioning

- To accurately capture the wave solution a mesh refinement of 10 elements per wavelength is usually used
- To stably discretise the operator product PA, the use of a dual mesh is required. The dual mesh is defined on the barycentrically refined original mesh leading to a 6-fold increase in the number of elements
- Applications have been limited to relatively small size parameters due to memory and time constraints.
- Accelerating techniques to reduce memory and assembly time

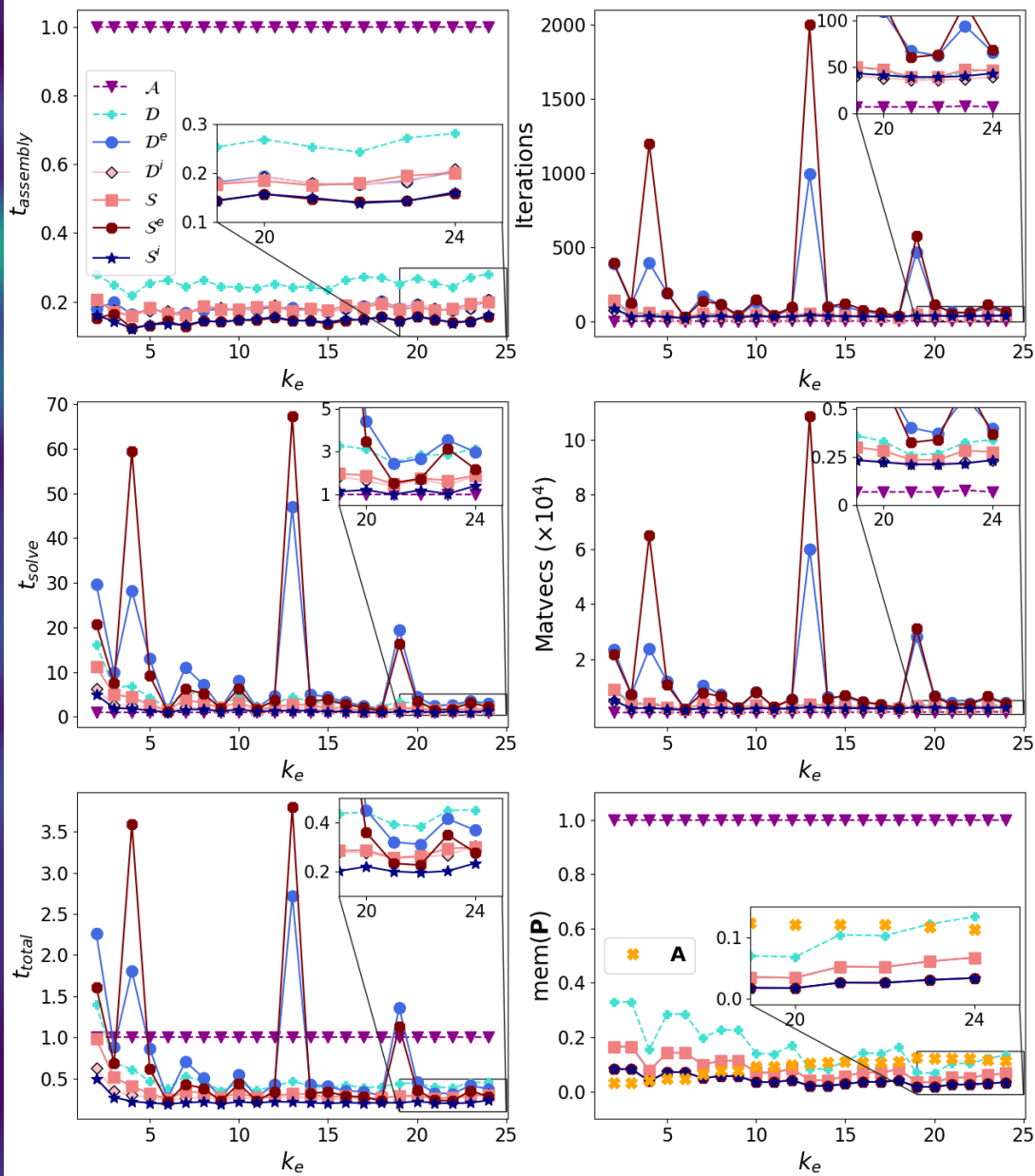
Kleanthous, Antigoni, et al. "Calderón preconditioning of PMCHWT boundary integral equations for scattering by multiple absorbing dielectric particles." Journal of Quantitative Spectroscopy and Radiative Transfer 224 (2019): 383-395.

Kleanthous, Antigoni, et al. "Accelerated Calderón preconditioning for Maxwell transmission problems." arXiv preprint arXiv:2008.04772 (2020).

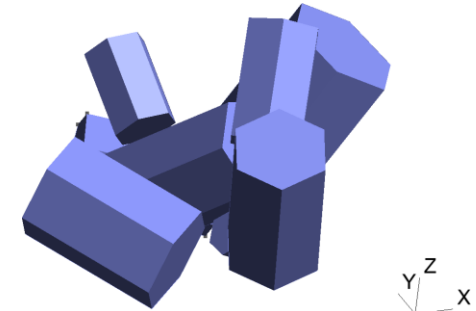
# Accelerated Preconditioning

$$\mathcal{A} = \begin{bmatrix} \mathcal{A}_1^e + \mathcal{A}_1^i & \mathcal{A}_{12} & & \cdots & \mathcal{A}_{1M} \\ \vdots & \ddots & \ddots & & \vdots \\ \mathcal{A}_{21} & \ddots & \ddots & \ddots & \vdots \\ \vdots & \ddots & \ddots & \ddots & \mathcal{A}_{(M-1)M} \\ \mathcal{A}_{M1} & \cdots & \mathcal{A}_{M(M-1)} & \mathcal{A}_M^e + \mathcal{A}_M^i & \end{bmatrix}$$

$$M = 3, \quad n = 1.0833 + 0.204i$$



# Accelerated Preconditioning

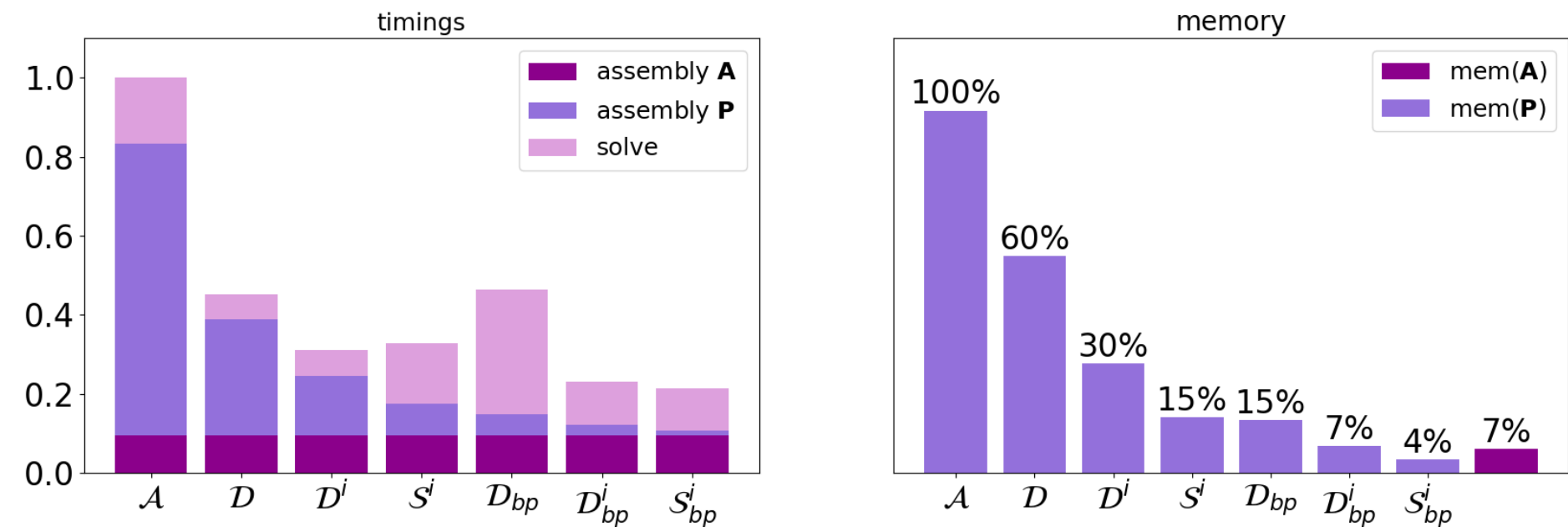


Frequency $f$	Refractive index $n$	Wavelength $\lambda_e$	Size parameter $\pi D_{max}/\lambda_e$	# dofs $N$
50 GHz	$1.7754 + 0.00066i$	0.60 cm	5	2556
183 GHz	$1.7754 + 0.00243i$	0.16 cm	20	26418
325 GHz	$1.7754 + 0.00440i$	0.092 cm	34	81318
664 GHz	$1.7754 + 0.00972i$	0.045 cm	70	332523

Yang, Ping, and K. N. Liou. "Single-scattering properties of complex ice crystals in terrestrial atmosphere." Beitrage zur Physik der Atmosphare-Contributions to Atmospheric Physics 71.2 (1998): 223-248.

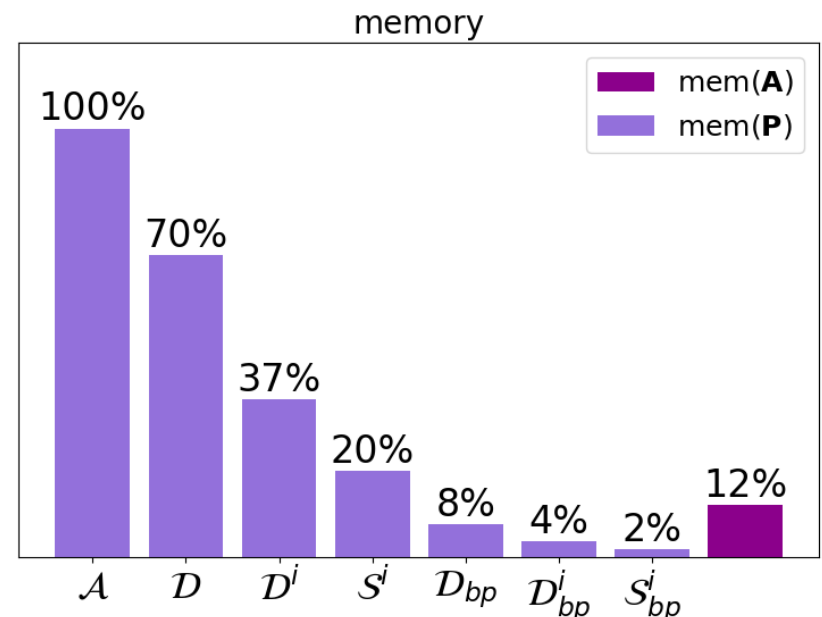
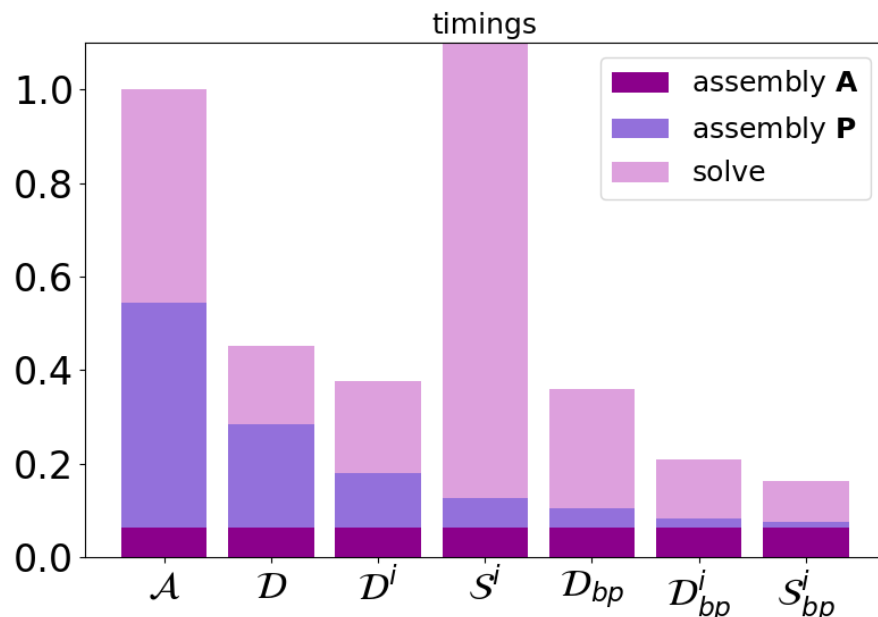
Kleanthous, Antigoni, et al. "Accelerated Calderón preconditioning for Maxwell transmission problems." arXiv preprint arXiv:2008.04772 (2020).

# Accelerated Preconditioning – 50GHz



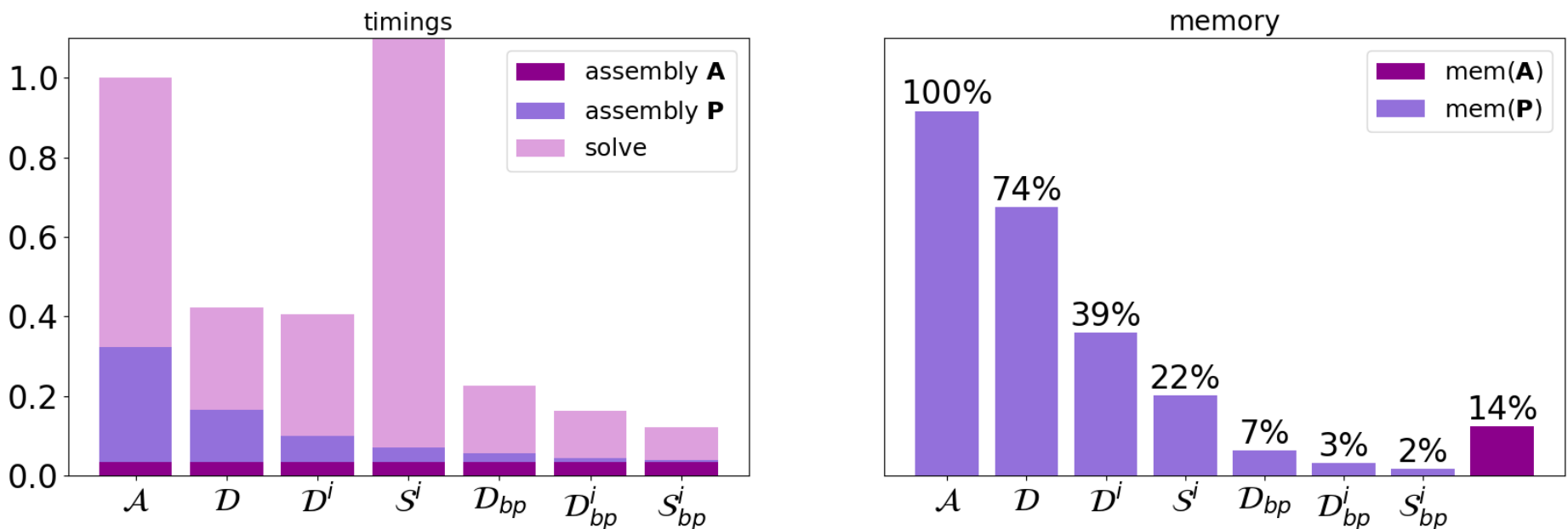
Kleanthous, Antigoni, et al. "Accelerated Calderón preconditioning for Maxwell transmission problems." arXiv preprint arXiv:2008.04772 (2020).

# Accelerated Preconditioning – 183GHz



Kleanthous, Antigoni, et al. "Accelerated Calderón preconditioning for Maxwell transmission problems." arXiv preprint arXiv:2008.04772 (2020).

# Accelerated Preconditioning – 325GHz

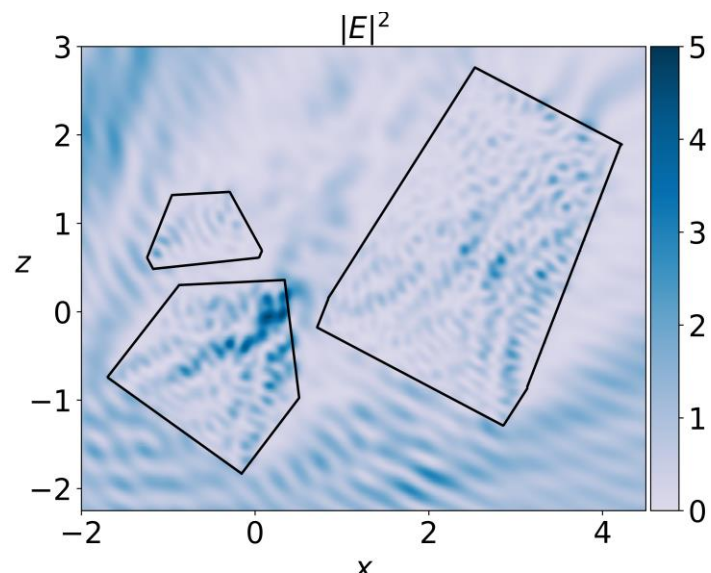
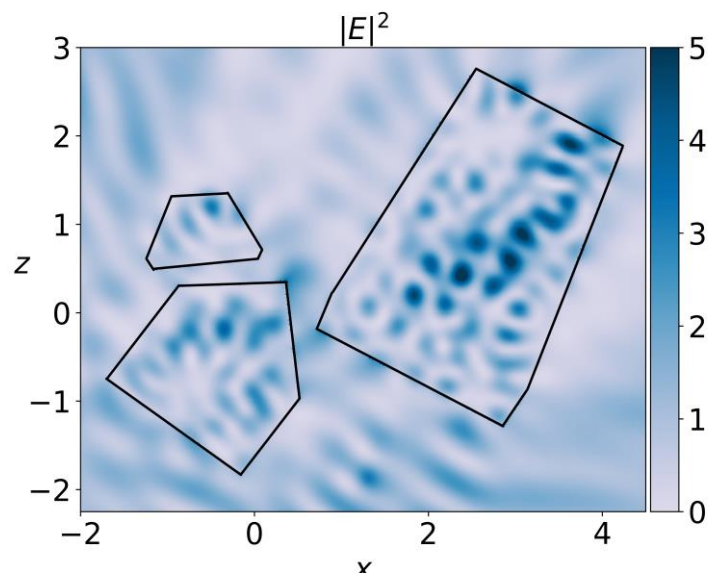
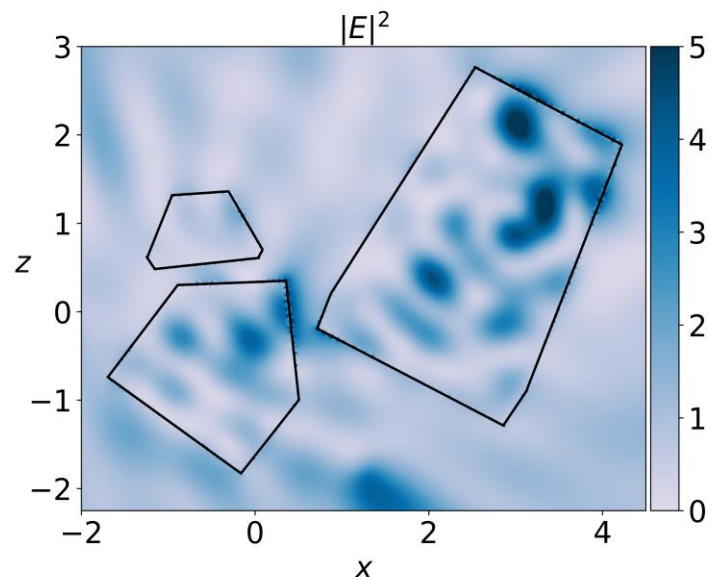
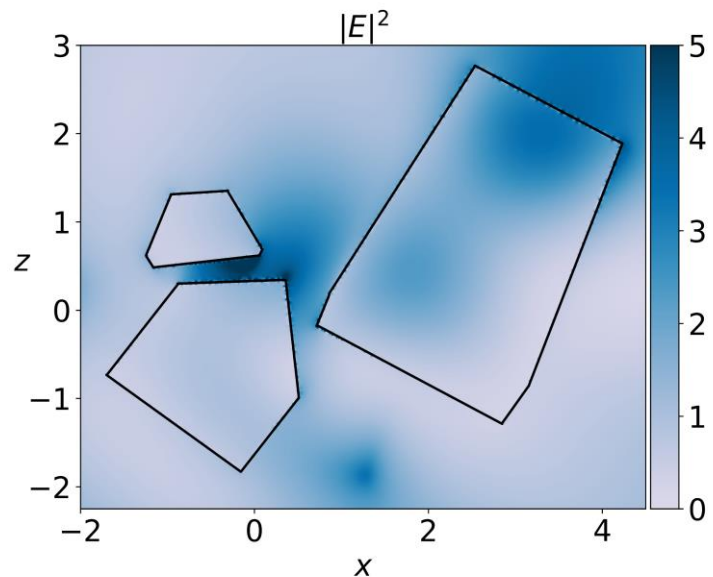


Kleanthous, Antigoni, et al. "Accelerated Calderón preconditioning for Maxwell transmission problems." arXiv preprint arXiv:2008.04772 (2020).

# Accelerated Preconditioning – 664GHz

- Unable to assemble the matrices except for  $S_{bp}^i$
- Assembly time:
  - 10 minutes for the preconditioner
  - 32 minutes for the operator
- GMRES time:
  - 62 minutes
  - 166 iterations
- Memory:
  - 9GB for preconditioner – estimated to be ~1-2% of the original non-accelerated version
  - 109GB for operator

Kleanthous, Antigoni, et al. "Accelerated Calderón preconditioning for Maxwell transmission problems." arXiv preprint arXiv:2008.04772 (2020).



Kleanthous, Antigoni, et al. "Accelerated Calderón preconditioning for Maxwell transmission problems." arXiv preprint arXiv:2008.04772 (2020).

## Part II: Using accelerated BEM for a microwave and sub-millimetre database

Antigoni Kleanthous, University College London, UK

Timo Betcke, University College London, UK

David Hewett, University College London, UK

Anthony Baran, The Met Office, UK & University of Hertfordshire, UK

Chris Westbrook, University of Reading, UK

# The database

- Goal: simulate SSPs and phase matrices of budding rosettes and aggregates of bullet rosettes in random orientation
- 5 temperatures: 190K, 210K, 230K, 250K, 270K
- 4 frequencies: 50GHz, 183GHz, 243GHz and 664GHz
- Range of sizes from  $\mu\text{m}$  to cm

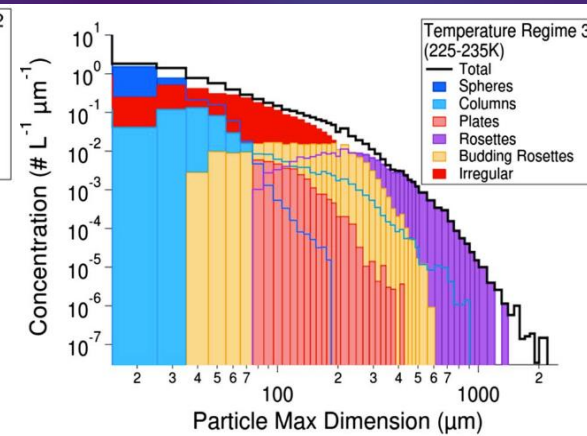
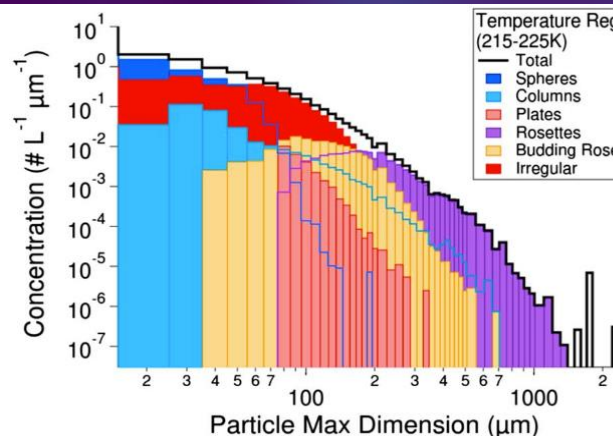
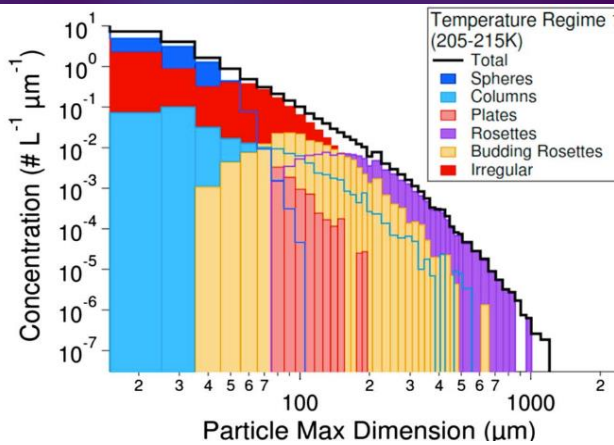
# The microphysical model

**Table A1**  
*Projects*

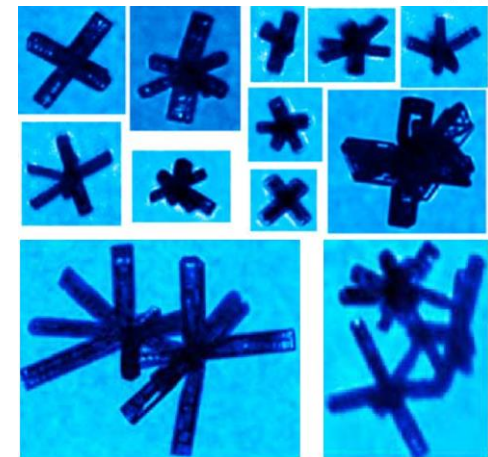
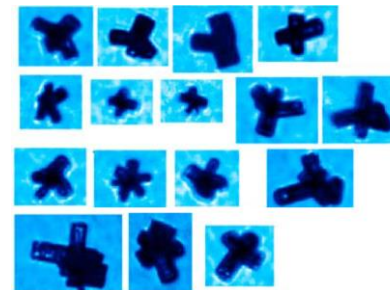
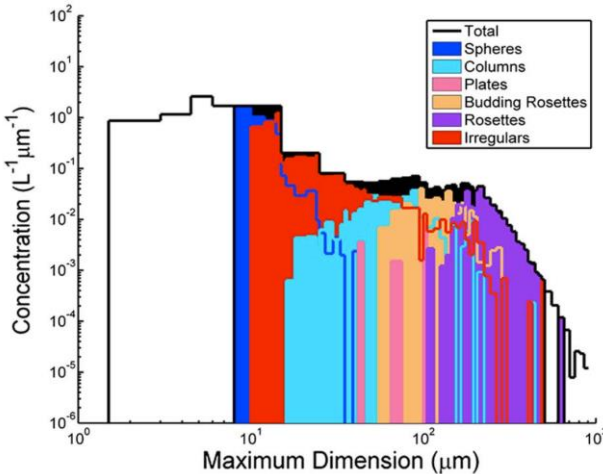
Acronym	Acronym expanded	Primary sponsor(s)
ACTIVE	Aerosol and Chemical Transport in Tropical Convection	UK NERC
ATTREX	Airborne Tropical Tropopause Experiment	NASA
CCOPE	Cooperative Convective Precipitation Experiment	NSF/BOR
CR-AVE	Costa Rica AURA Validation Experiment	NASA
CRYSTAL-FACE	Cirrus Regional Study of Tropical Anvils and Cirrus Layers-Florida Area Cumulus Experiment	NASA
DC3	Deep Convective Clouds and Chemistry Project	NASA/NSF
EOS	Earth Observing System	DOE
EMERALD-I & II	Egrett Microphysics Experiment with Radiation, Lidar, and Dynamics	UK NERC
FIRE.ACE	First ISCCP Regional Experiment Arctic Cloud Experiment	NASA/DOE
FIRE-II	First ISCCP Regional Experiment	NASA
ICE-T	Ice in Clouds Experiment-Tropical	NSF
ISDAC	Indirect and Semi-Direct Aerosol Campaign	DOE, NASA
MIDCIX	Midlatitude Cirrus Cloud Experiment	DOE
POSIDON	Pacific Oxidants, Sulfur, Ice, Dehydration, and Convection Experiment	NASA
SEAC4RS	Studies of Emissions and Atmospheric Composition, Clouds and Climate Coupling by Regional Surveys	NASA
SCCP	Sierra Cooperative Pilot Project	BOR
SPARTICUS	Small Particles in Cirrus Project	DOE
TC4	Tropical Composition, Cloud and Climate Coupling	NASA
TRMM KWAJEX	Tropical Rain Measurement Mission Kwajalein Experiment	NASA
TRMM TEFLUN-A	TRMM Texas and Florida Under Flights – A (Texas)	NASA
TRMM TEFLUN-B	TRMM Texas and Florida Under Flights – B (Florida)	NASA
TWP-ICE	Tropical Warm Pool – International Cloud Experiment	DOE

Lawson, R. P., et al. "A review of ice particle shapes in cirrus formed in situ and in anvils." Journal of Geophysical Research: Atmospheres 124.17-18 (2019): 10049-10090.

# The microphysical model



## In Situ Cirrus



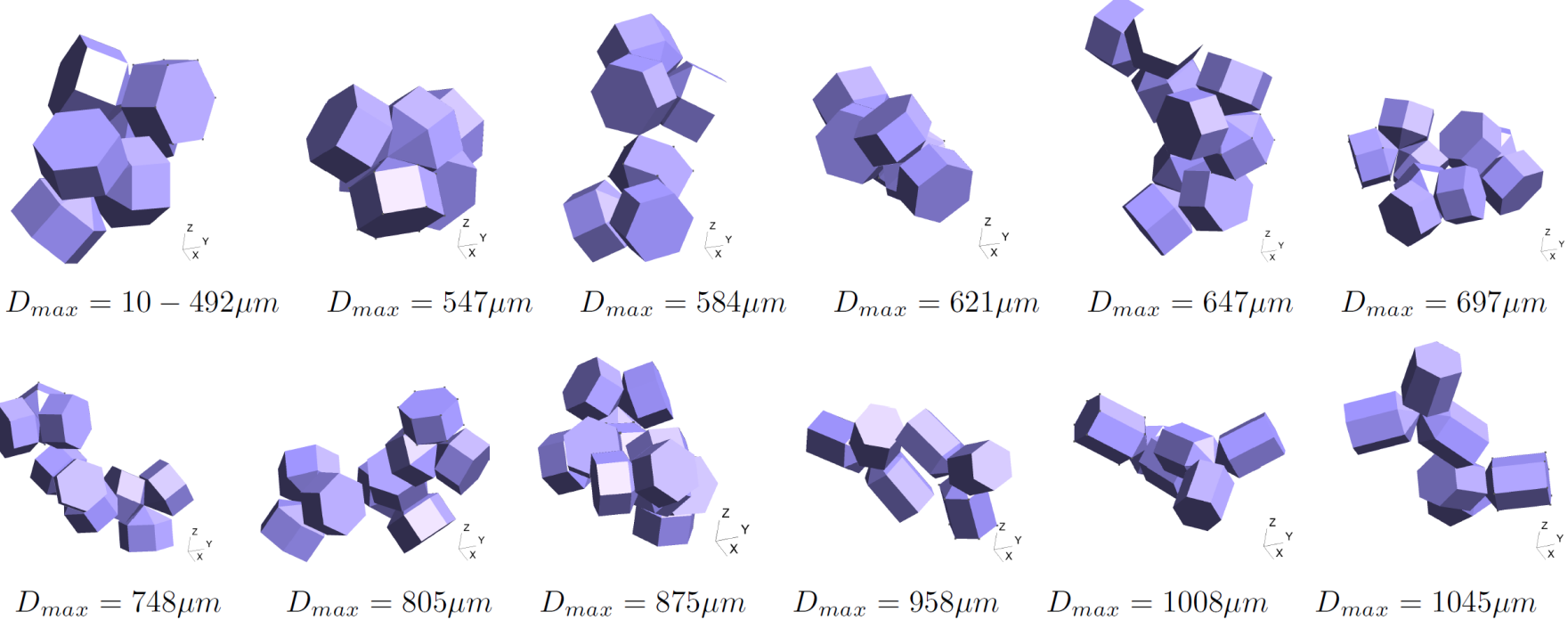
Lawson, R. P., et al. "A review of ice particle shapes in cirrus formed in situ and in anvils." Journal of Geophysical Research: Atmospheres 124.17-18 (2019): 10049-10090.

# The microphysical model

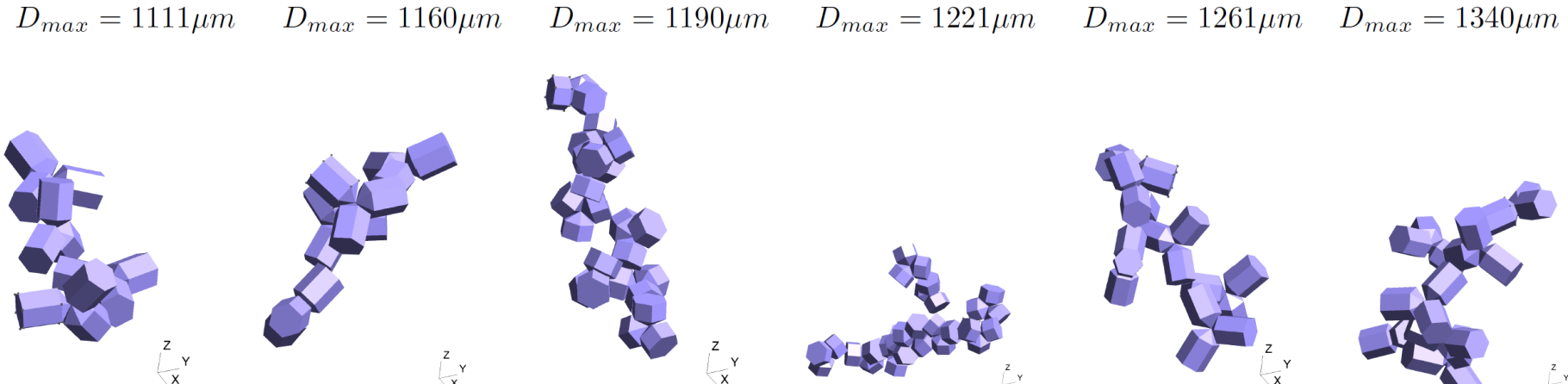
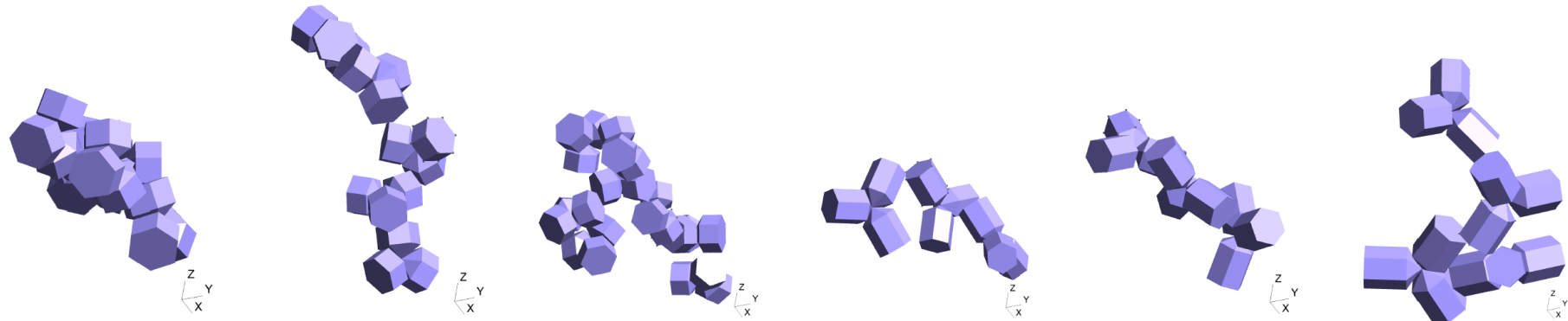
- The aggregates were generated using the ice aggregation model of (Westbrook, et al., 2004) formed by Monte Carlo simulations
- The monomer rosettes are constructed of three-branched rosettes, which are aggregated together to follow the Cotton et al. mass–dimension relationship – to be consistent with the Unified Model used at the Met Office
- Each of the monomers that makes up the ensemble of rosette aggregates is assumed to have the density of solid ice,  $917 \text{ kg/m}^3$
- The final model consists of 65 aggregates, of maximum dimension between 10 and  $10,000\mu\text{m}$ .

Westbrook, C. D., et al. "Theory of growth by differential sedimentation, with application to snowflake formation." Physical Review E 70.2 (2004): 021403.

# The microphysical model



# The microphysical model



$D_{max} = 1422\mu m$

$D_{max} = 1461\mu m$

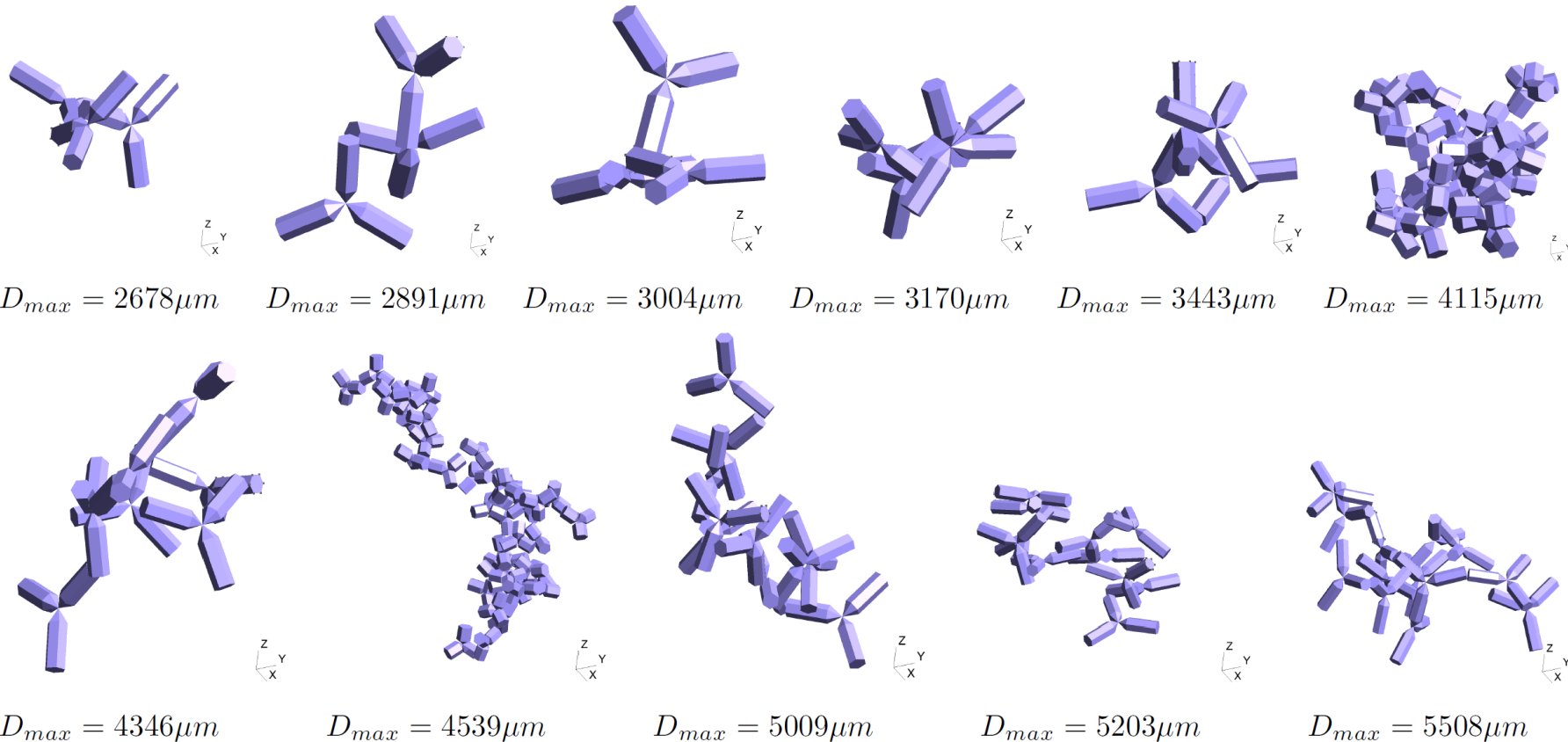
$D_{max} = 1510\mu m$

$D_{max} = 1630\mu m$

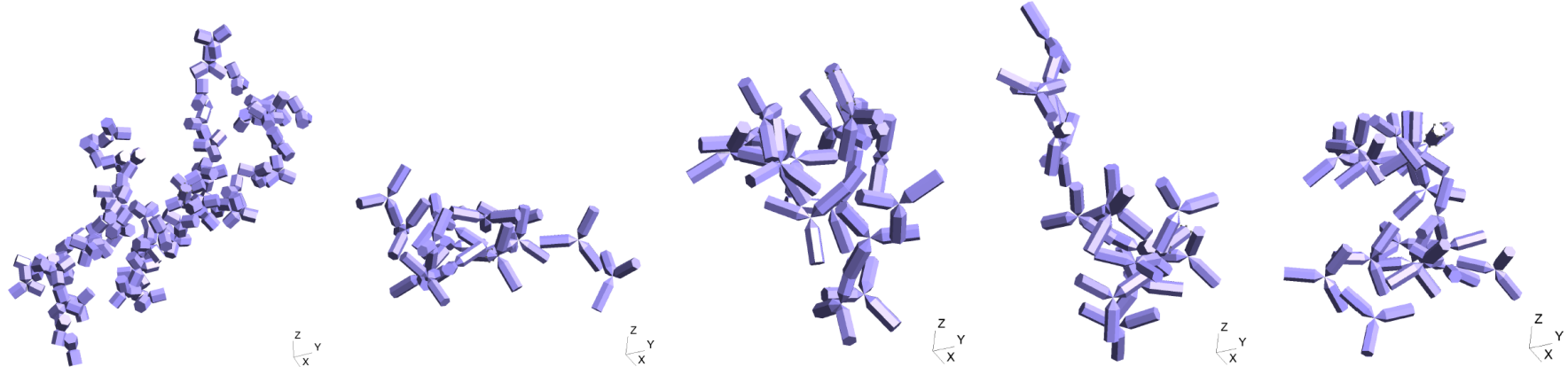
$D_{max} = 1700\mu m$

$D_{max} = 1759\mu m$

# The microphysical model



# The microphysical model



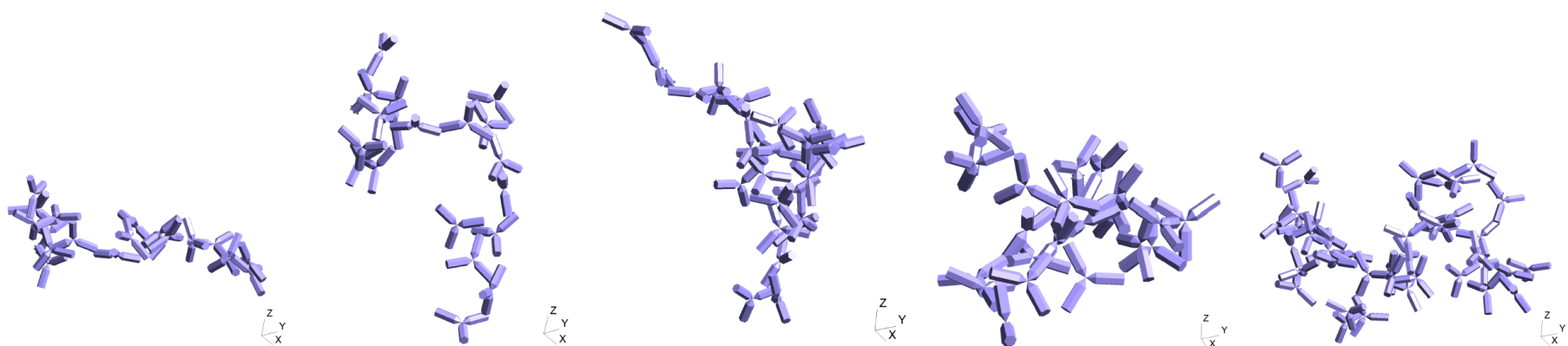
$D_{max} = 5791\mu m$

$D_{max} = 6188\mu m$

$D_{max} = 6456\mu m$

$D_{max} = 6688\mu m$

$D_{max} = 6881\mu m$



$D_{max} = 7884\mu m$

$D_{max} = 8582\mu m$

$D_{max} = 9200\mu m$

$D_{max} = 9594\mu m$

$D_{max} = 10235\mu m$

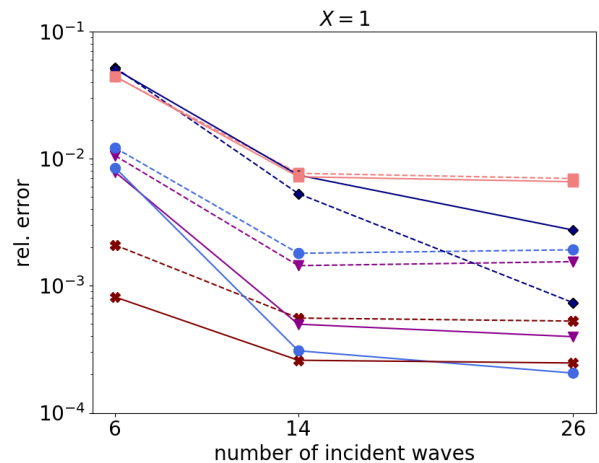
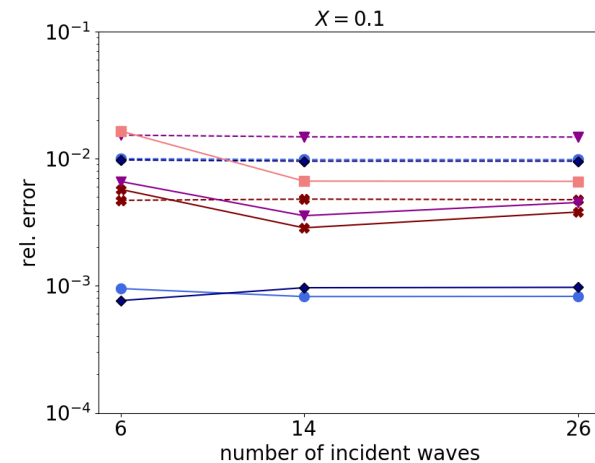
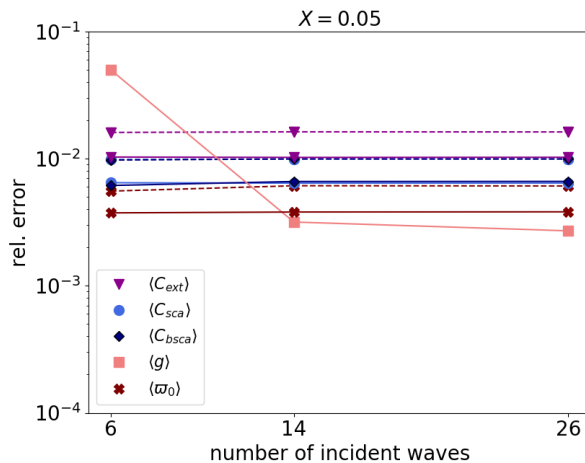
# Simulating random orientation

- The orientation average of some quantity is evaluated by a triple integral over the three Euler angles used to describe the orientation of a body
- The traditional approach to achieve this is to fix the direction of the incident wave, and then rotate the particle in three directions via the three Euler angles. The SSPs and phase matrix are then evaluated for some scattering angles.

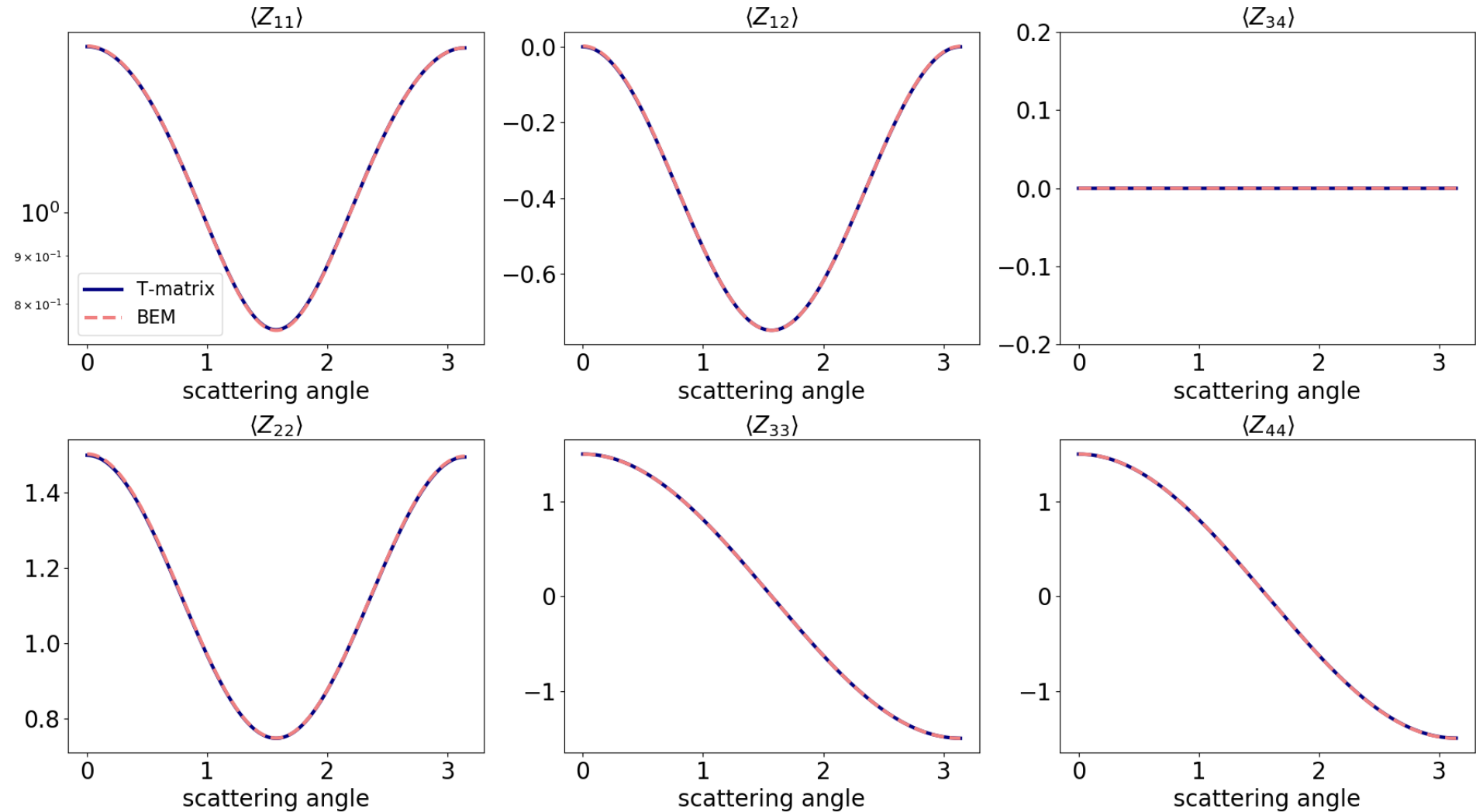
# Simulating random orientation

- The traditional approach would be too expensive to follow using BEM: each rotation requires the assembly of a new matrix operator and preconditioner.
- Fixing the direction of the incident wave and rotating the scatterer by the appropriate rotation matrix is equivalent to fixing the orientation of the scatterer and instead rotating the direction and polarisation vectors of the incident wave by the inverse rotation matrix.
- This enables us to assemble the operator matrix and preconditioner once and re-use for all incident wave solutions. By using appropriate quadrature schemes suitable for numerical integration over a sphere our integration scheme reduces to only 2 loops; a combination of Lebedev and Gaussian quadrature.
- In addition, the different incoming waves are distributed over different CPUs to accelerate solution even further.

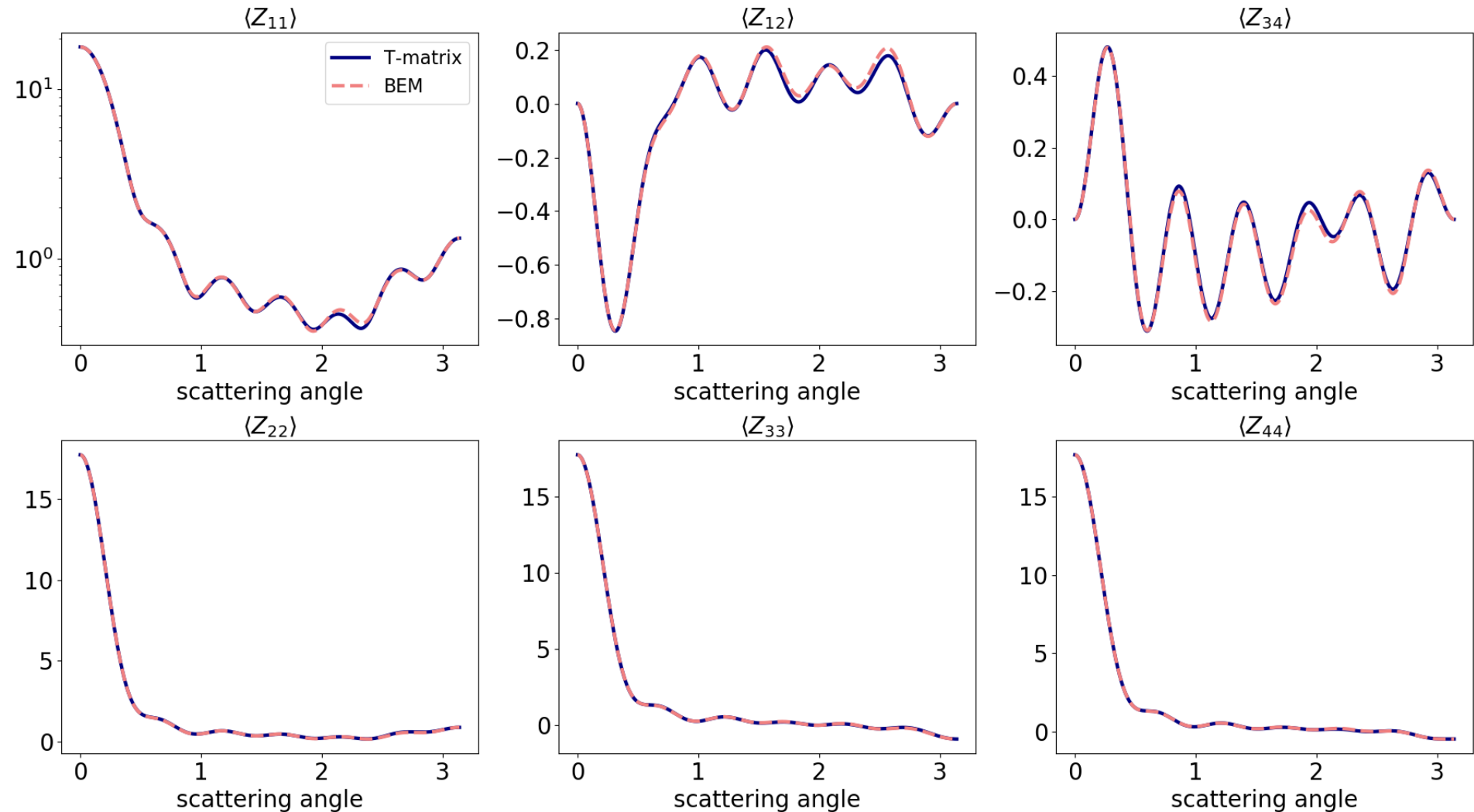
# Testing our method



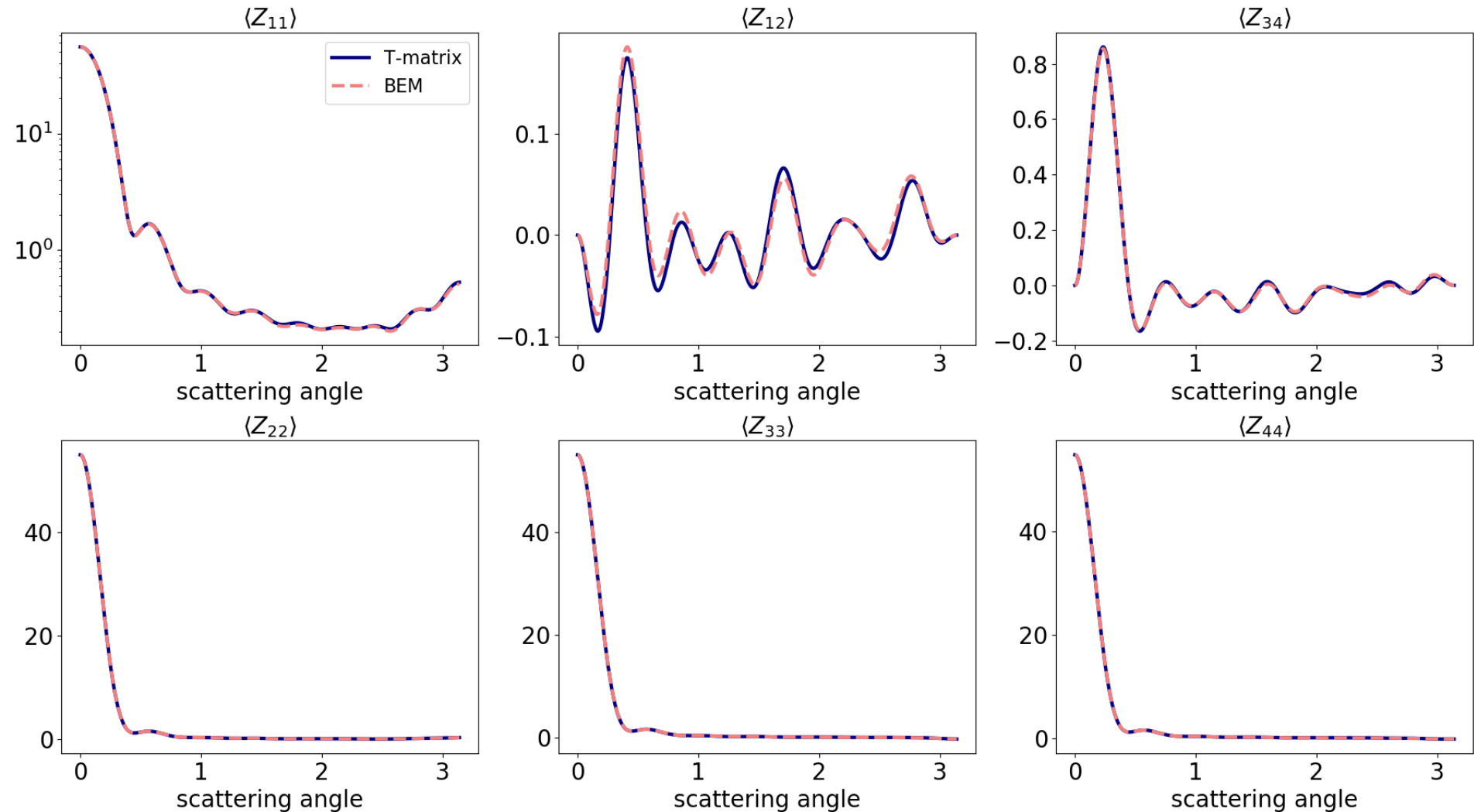
# Testing our method – X=0.05



# Testing our method – X=5



# Testing our method – X=10



# Testing our method

- To obtain SSPs to within accuracies of 10% or so, (Liu, et al., 2008), using the discrete dipole approximation (DDA), found that  $17 \times 16 \times 16$  (4352) orientations were required to simulate random orientation.
- With our method we can reduce the number of incident waves and rotations of the polarisation vectors needed depending on the size parameter of the aggregate.
- To accurately compute the SSPs within accuracy of 1-5% we need
  - $X < 1$ : 14 incident directions
  - $1 < X < 3$ : 50 incident waves
  - $3 < X < 5$ : 110 incident waves
  - $5 < X < 8$ : 194 incident waves
  - $8 < X < 10$ : 230 incident waves
  - $X > 10$ : 302 incident waves
- To obtain the phase matrix to 1-2% relative error we also need:
  - $X < 1$ : 10 rotations of the polarisation vectors
  - $1 < X < 24$ : 15 rotations of the polarisation vectors
  - $X > 24$ : 20 rotations of the polarisation vectors

# Part III: Scattering by inhomogeneous particles

Antigoni Kleanthous, University College London, UK

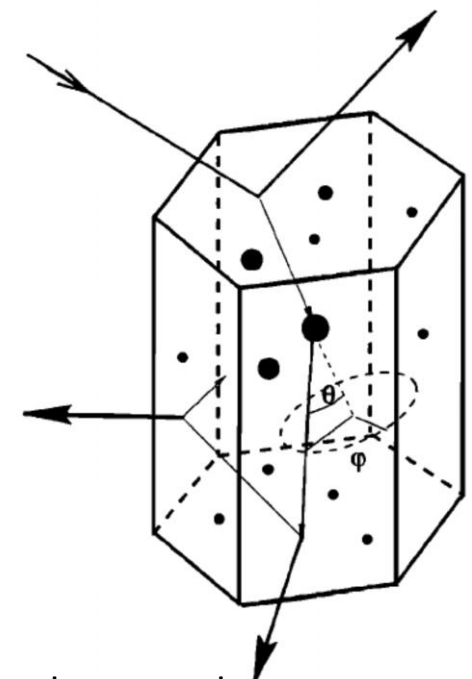
Timo Betcke, University College London, UK

David Hewett, University College London, UK

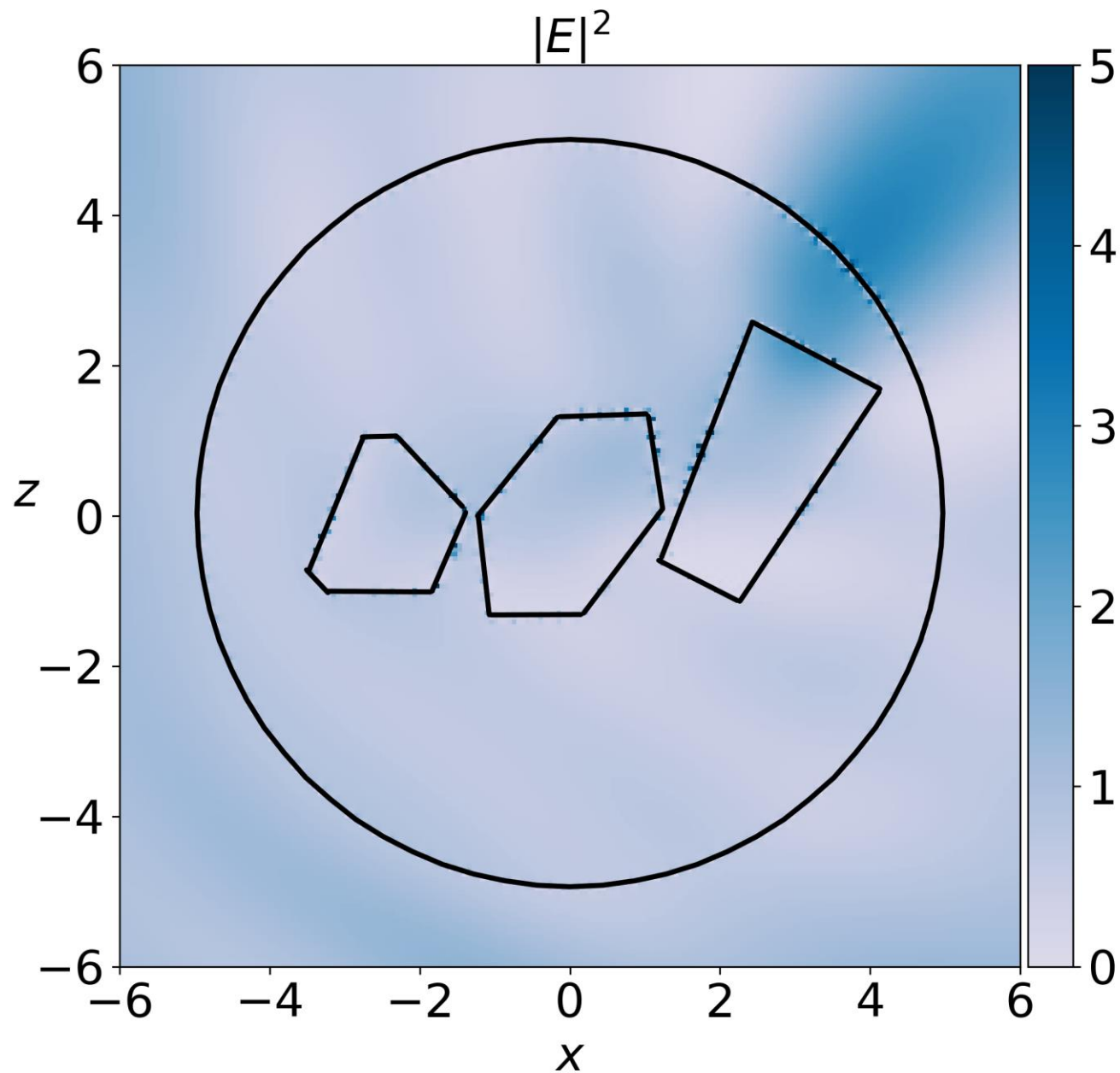
Anthony Baran, The Met Office, UK & University of Hertfordshire, UK

# Inhomogeneous scatterers

- The boundary integral formulation and preconditioning can be easily extended to simulate scattering by inhomogeneous scatterers
  - Hexagonal columns with air bubbles
  - Ice crystal in a liquid droplet



C.-Labonnote, Laurent, et al. "Polarized light scattering by inhomogeneous hexagonal monocrystals: Validation with ADEOS-POLDER measurements." Journal of Geophysical Research: Atmospheres 106.D11 (2001): 12139-12153.



# Future Steps

- Complete simulations for the database to include phase matrix calculations
- Time permitting, explore scattering by inhomogeneous scatterers